eLIFE elifesciences.org

RESEARCH ARTICLE

Figures and figure supplements

The RNA helicase UPF1 associates with mRNAs co-transcriptionally and is required for the release of mRNAs from gene loci

Anand K Singh *et al*

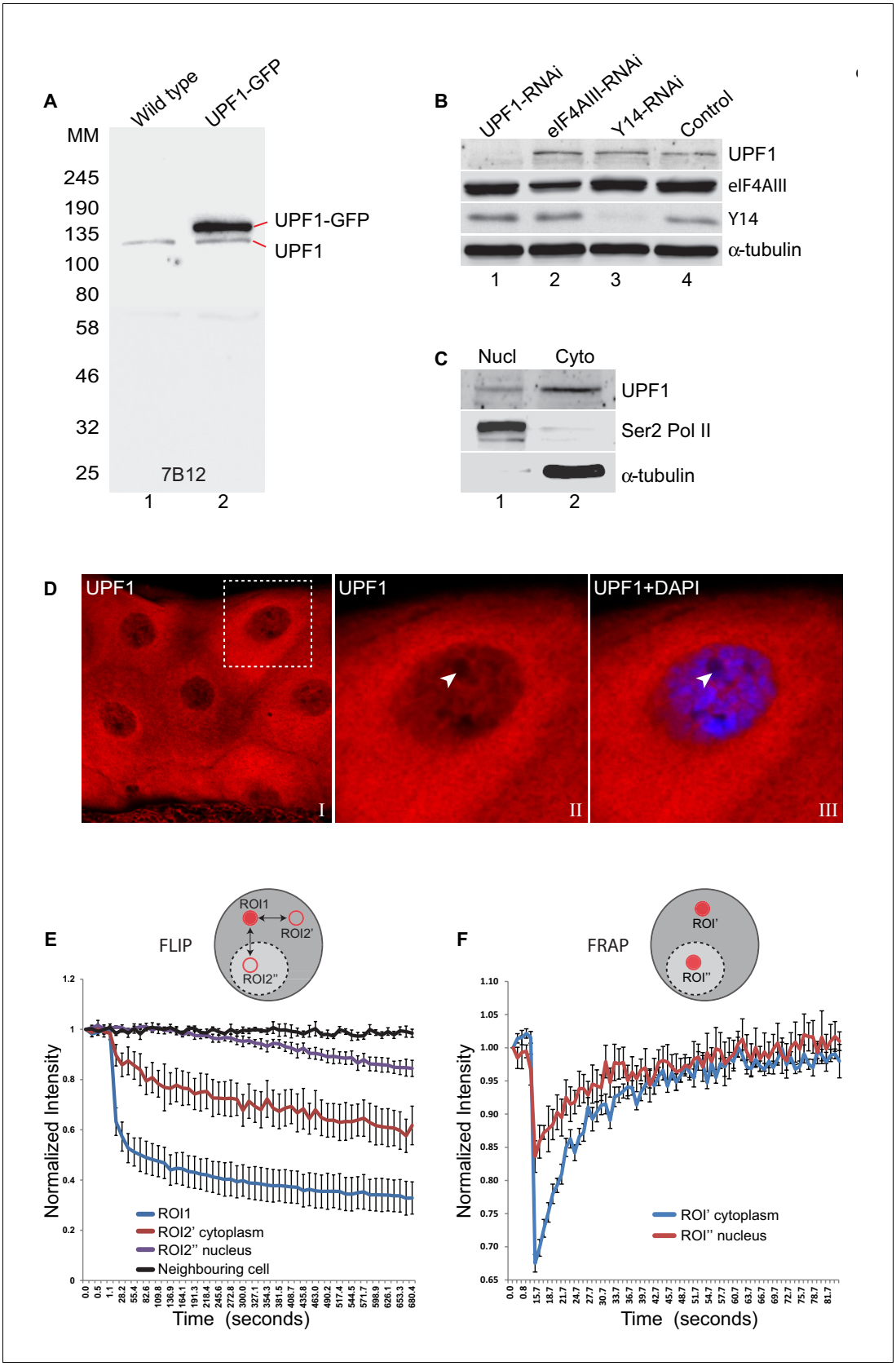

Figure 1. UPF1 continuously shuttles between nucleus and cytoplasm. (**A**) Western blotting of whole-cell lysate from either normal (lane 1) or transfected S2 cells expressing UPF1-GFP (lane 2), probed with the UPF1 monoclonal antibody 7B12. The proteins run according to their expected

Figure 1 continued on next page

Figure 1 continued

molecular weights: UPF1 (~130 kDa), and UPF1-GFP (~157 kDa) (**B**) Western blotting of S2 cells treated with dsRNA targeting UPF1 or other RNA binding proteins indicated, used as controls. Different sections of the membrane were probed with anti-UPF1 (7B12, top row), anti-eIF4AIII (row 2), anti-Y14 (row 3) or anti-α-tubulin (row 4) as a loading control. (**C**) Western blotting of UPF1 following nuclear (Nucl) and cytoplasmic (Cyto) fractionation of S2 cells. RNA Pol II and α-tubulin were detected using the corresponding antibodies on the same blot (shown below). (**D**) Fluorescence immunolocalisation of UPF1 (Cy3, red) in third instar larval salivary gland. The arrowheads in panel II and III (magnified view of boxed area in panel I) point to the nucleolus, identified by no DAPI staining, which, as other nucleoli, shows no UPF1 signal in its centre. (**E**) The plot shows fluorescence loss in photobleaching (FLIP) of GFP-UPF1in salivary gland cells photobleached in ROI1 (red circle, cytoplasm) and then GFP signal measured at the identical time points in two separate ROI2s (red rings), in either cytoplasm or nucleus; both equidistant from ROI1. The different lines show rate of GFP fluorescence loss in either the photobleached ROI1 (blue line), or ROI2' in the cytoplasm (red line) or ROI2'' in nucleus (purple line). Change in fluorescence intensity at equivalent regions in neighbouring cells was measured as a control during the same time-course (black line). Y-axis shows normalised relative fluorescence intensity while X-axis shows time (seconds) from the start of imaging. Quantification based on imaging experiments in eight different cells. (**F**) Plot shows fluorescence recovery after photobleaching (FRAP) of GFP-UPF1 in either cytoplasm (ROI', blue line) or nucleus (ROI'', red line) of salivary gland cells. Line values represent the average of eight separate measurements in different cells. Error bars in E and F indicate ±Standard Error.

DOI: https://doi.org/10.7554/eLife.41444.002

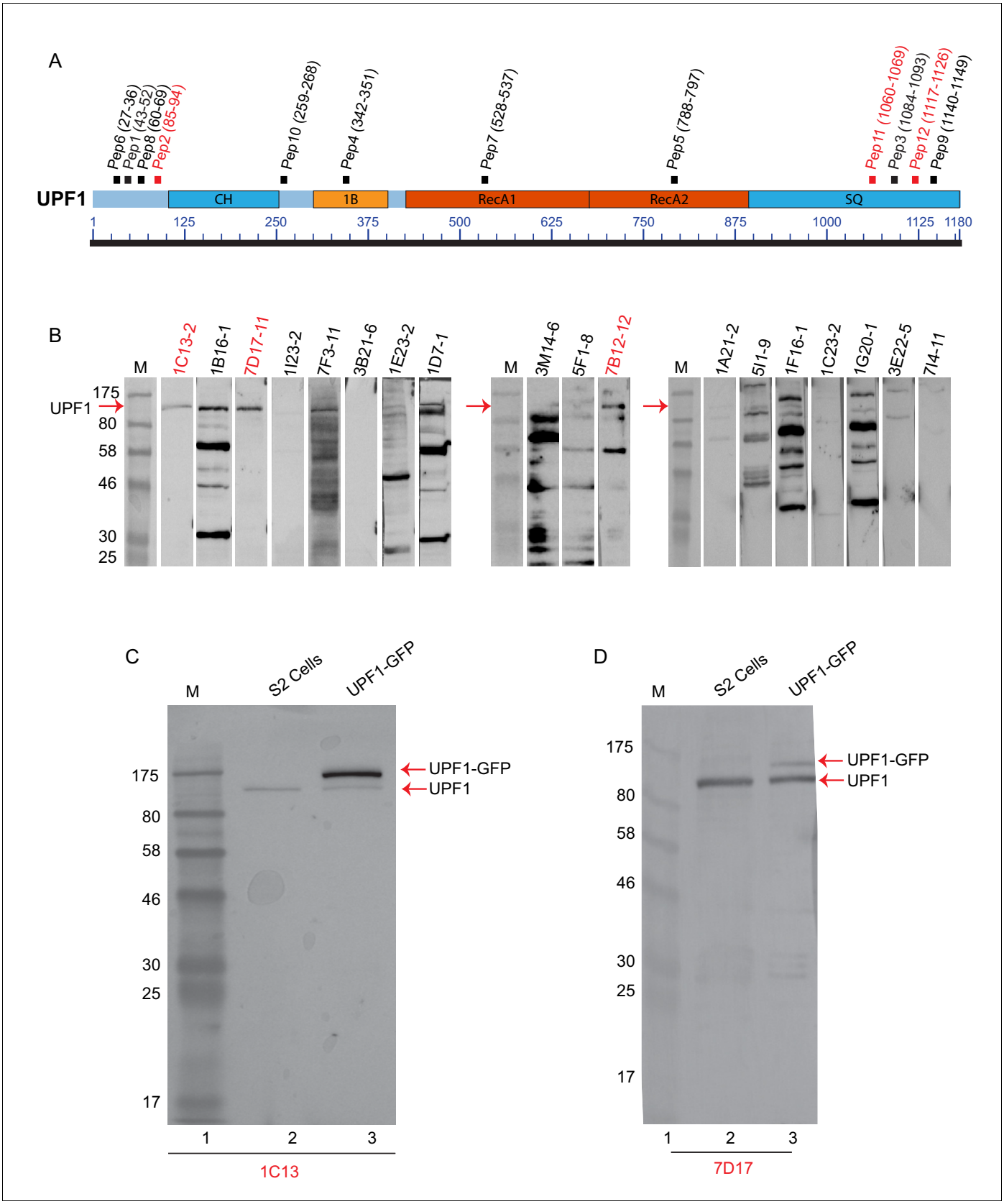

Figure 1—figure supplement 1. Generation of monoclonal antibodies against Drosophila UPF1. (**A**) Schematics of UPF1 showing its different structural domains. The peptides used as immunogens and their respective amino acid locations are given in brackets (sequences are in ***Supplementary file 1***).

Figure 1—figure supplement 1 continued on next page

Figure 1—figure supplement 1 continued

The peptides indicated by red colour produced the monoclonal antibodies with highest specificity, as shown below (**B**) Western blotting of S2 cell protein extracts, probed with 18 ascites induced with hybridomas previously screened for their reactivity to the corresponding peptides (terminal numbers correspond to different peptides indicated in A). Lanes labelled M show a molecular weight marker. (**C**) Western blotting of whole-cell lysate with the UPF1 monoclonal antibody (mab) 1C13, purified from hybridoma supernatants, from either normal (lane 2) or transfected S2 cells expressing UPF1-GFP (lane 3) in which the two bands correspond to either endogenous UPF1 or UPF1-GFP. (**D**) As in C, using mab 7D17. Western blotting with 7B12 is shown in ***Figure 1A***.

DOI: https://doi.org/10.7554/eLife.41444.003

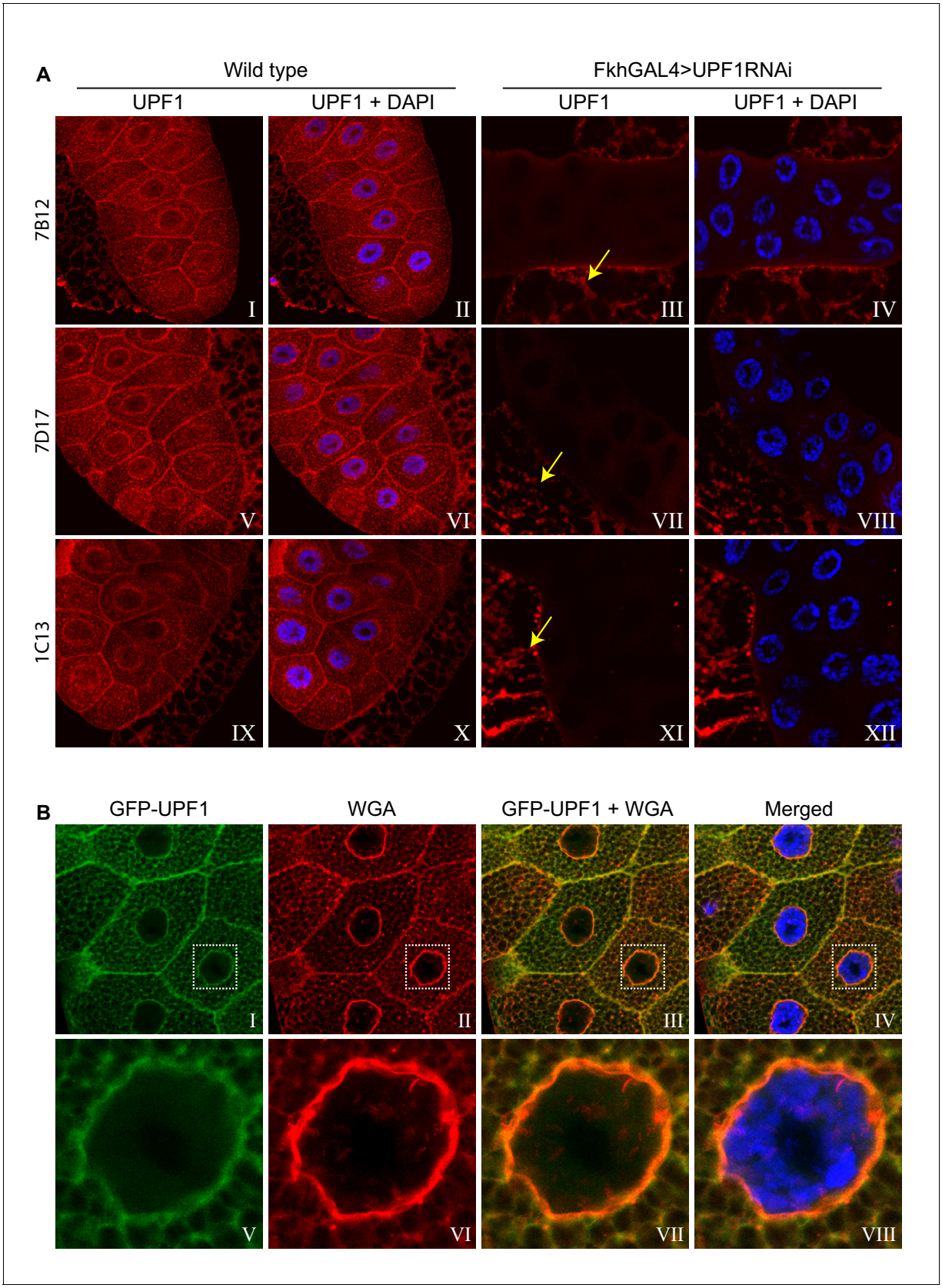

Figure 1—figure supplement 2. UPF1 immunostaining signals are reduced in UPF1-RNAi salivary glands. (**A**) Fluorescence immunolocalisation of UPF1 (Cy3, red) in third instar larval salivary gland, using three different antibodies: 7B12 (**I to IV**), 7D17 (**V to VIII**) or 1C13 (**IX to XII**) in either wild-type (left

Figure 1—figure supplement 2 continued on next page

Figure 1—figure supplement 2 continued

panels) or FkhGAL4 >UPF1 RNAi (right panels). Yellow arrows in III, VII and XI are indicating the fat body associated with corresponding salivary glands. Nuclei were counter-stained with DAPI (blue). (**B**) Colocalisation of transgenic GFP-UPF1 (green) and tetramethylrhodamine conjugated Wheat Germ Agglutinin (WGA, red) in salivary gland cells. Lower panels are magnified views of boxed area in upper panel.

DOI: https://doi.org/10.7554/eLife.41444.004

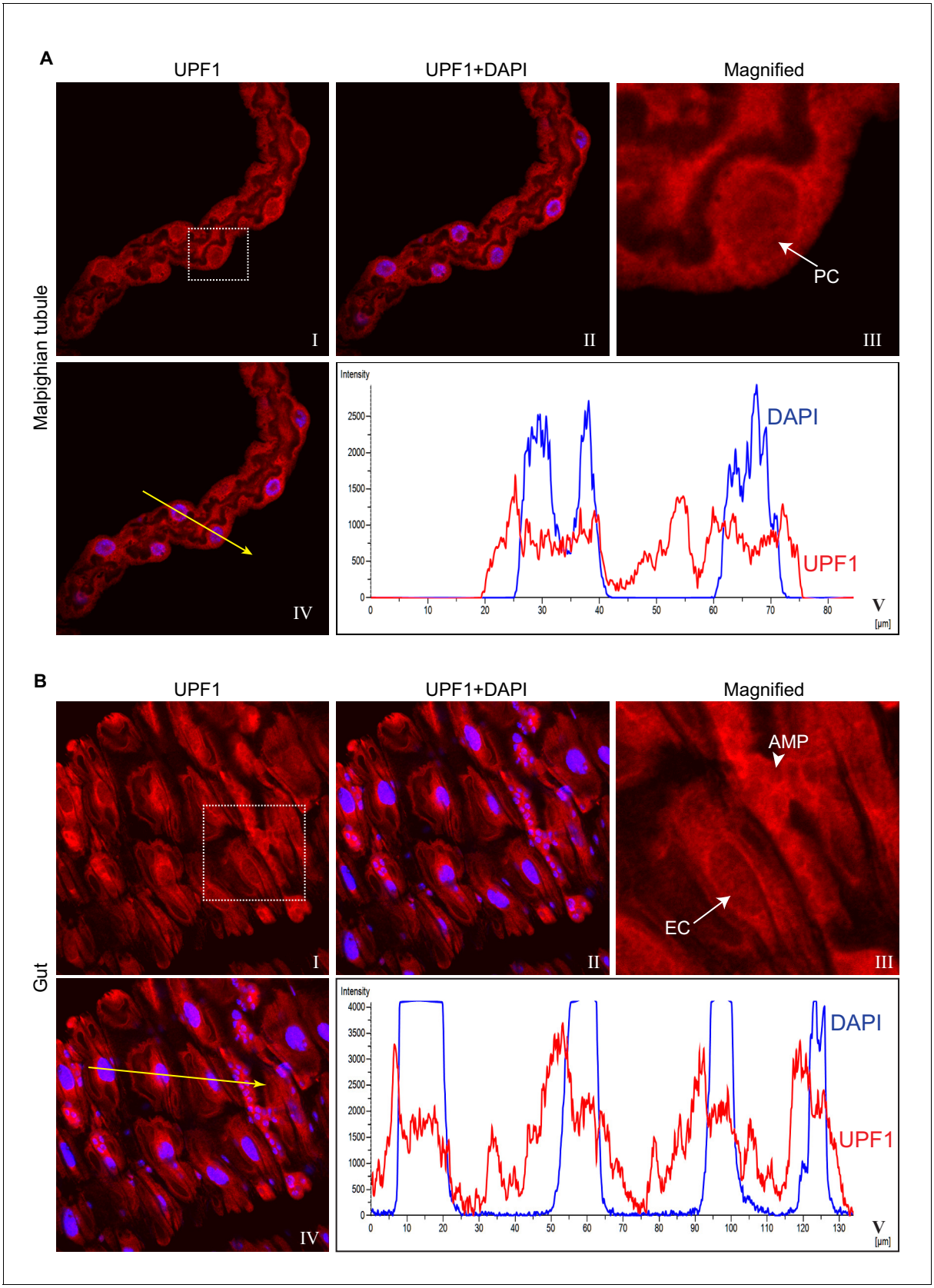

Figure 1—figure supplement 3. UPF1 subcellular localisation in different larval tissues. (**A**) Fluorescence immunolocalisation of UPF1 (Cy3, red) in third instar larval Malpighian tubule (**I to IV**). Panel III shows magnified view of boxed area in panel I, where white arrow indicates UPF1 signal within nucleus

Figure 1—figure supplement 3 continued on next page

Figure 1—figure supplement 3 continued

of a Principal Cell (PC). Tissues were counter-stained with DAPI (blue). Line profiles (**V**) show both Cy3 and DAPI fluorescence intensities along the yellow line drawn (**IV**). (**B**) Immunolocalisation of UPF1 (Cy3, red) in gut cells (**I to IV**). Panel III shows magnified view of boxed area in panel I. Arrow and arrowhead in (**III**) indicate presence of UPF1 within nuclei of Enterocytes Cell (EC) and Adult Midgut Progenitor Cells (AMPs) respectively. The line profiles show both Cy3 and DAPI fluorescence intensities along the yellow line (**IV**) across both EC and AMPs cells (**V**).

DOI: https://doi.org/10.7554/eLife.41444.005

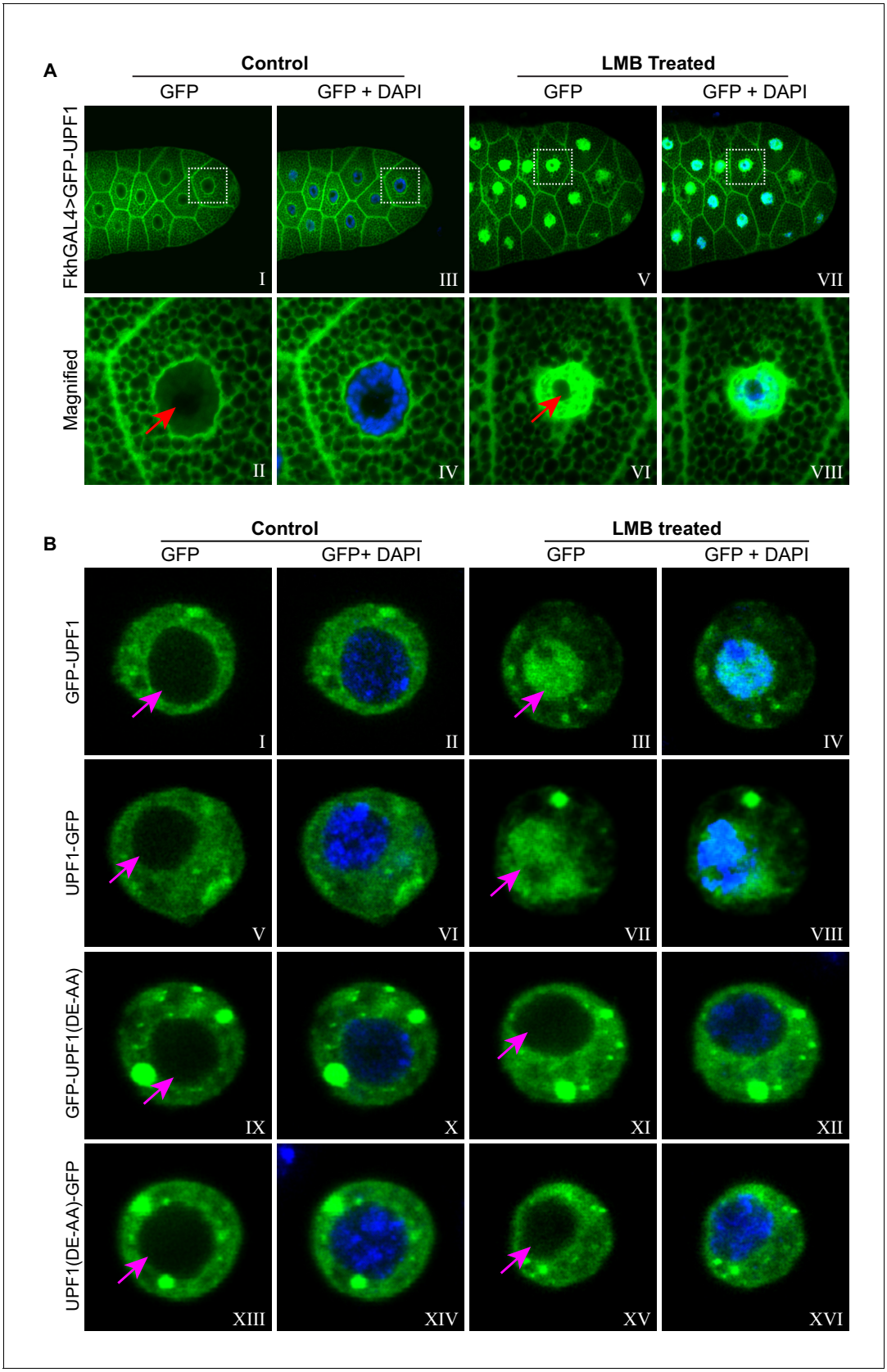

Figure 2. UPF1 shuttling between nucleus and cytoplasm requires its RNA helicase activity. (**A**) Imaging of third instar larval salivary glands over-expressing GFP-UPF1 (green), incubated for 1 hr in either normal M3 media (Control, **I to IV**) or supplemented with 50 nM LMB (LMB, **V to VIII**). Panels

Figure 2 continued on next page

Figure 2 continued

II, IV, VI and VIII are magnified views of the boxed areas in panel I, III, V and VII, respectively. The red arrows in II and VI indicate the nucleoli. Nuclei were counter-stained with DAPI (blue). (**B**) Imaging of transfected Drosophila S2 cells expressing either GFP-UPF1 (**I to IV**), UPF1-GFP (**V to VIII**), GFP-UPF1(DE-AA) (**IX to XII**) or UPF1(DE-AA)-GFP (**XIII to XVI**), incubated for 1 hr with or without 50 nM LMB (right vs. left panels). The magenta coloured arrows indicate the nuclei, which were counter-stained with DAPI (blue) in the even numbered panels.

DOI: https://doi.org/10.7554/eLife.41444.006

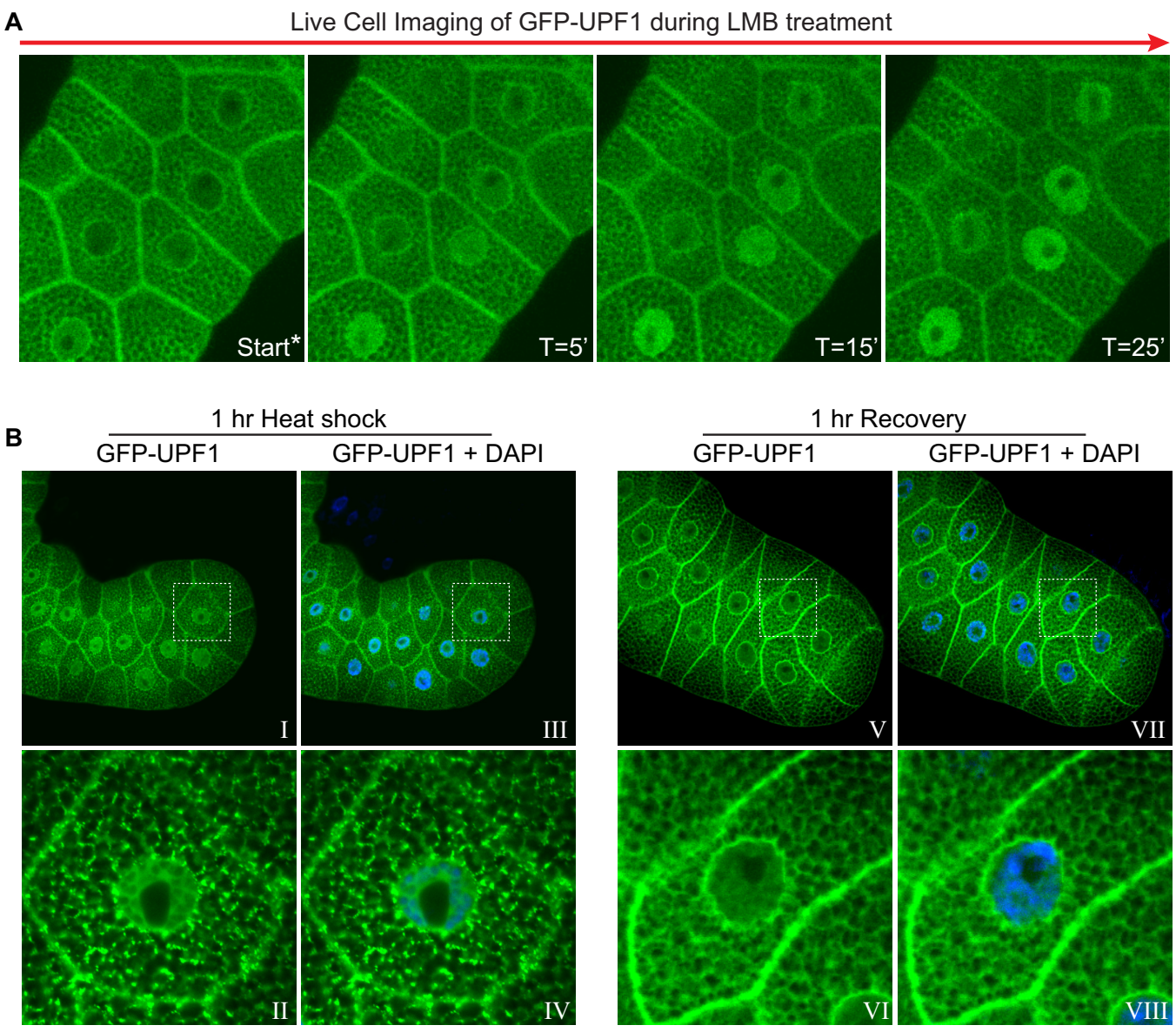

Figure 2—figure supplement 1. UPF1 is highly dynamic within both nucleus and cytoplasm. (**A**) Time-lapse live cell imaging showing changes in the cellular distribution of GFP-UPF1 in third instar larval salivary gland at different time intervals of LMB treatment. Start* refers to the first image acquired straight after dissection and mounting of the tissues in a cavity slide, the procedure takes ~5–6 min during which time the cells have been exposed to LMB. (**B**) Localisation of GFP-UPF1 (green) in salivary glands either after 1 hr heat shock (**I to IV**) or after a further 1 hr recovery following heat shock (**V to VIII**). Lower panels are magnified views of boxed area in upper panel, with or without DAPI counter-staining (blue).

DOI: https://doi.org/10.7554/eLife.41444.007

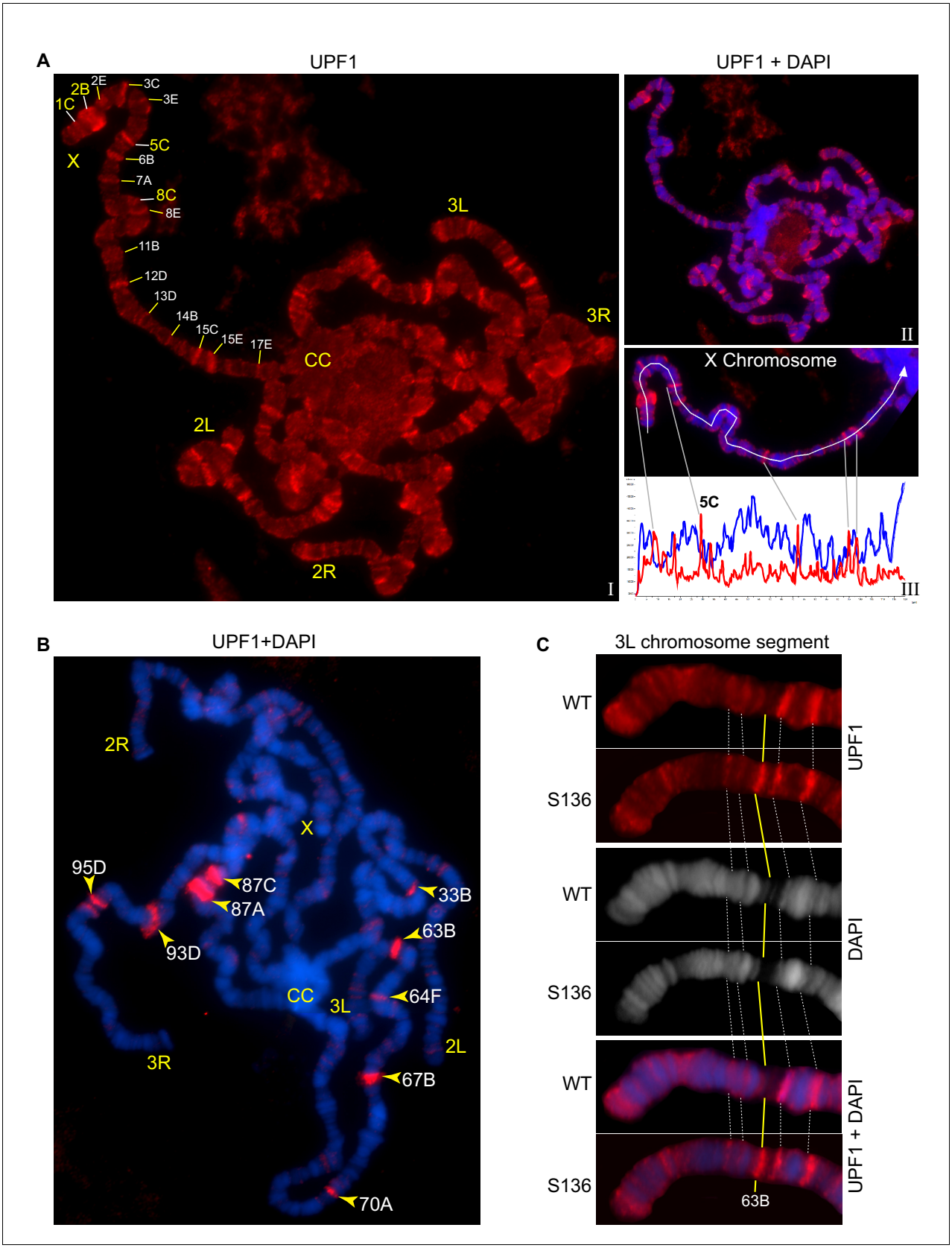

Figure 3. UPF1 binds at transcriptionally active sites on the polytene chromosomes. (**A**) Fluorescence immunolocalisation of UPF1 (Cy3, red, (**I**) on polytene chromosomes (DAPI, blue, **II**). Chromosome arms (X, 2L, 2R, 3L and 3R) and chromocentre (CC) are labelled. The labels indicate cytological

Figure 3 continued on next page

Figure 3 continued

locations of interband regions at the X chromosome, presenting apparent UPF1 signal. The line profile (**III**, white panel) shows signal intensities along the white line drawn on the X chromosome, UPF1 (red) and DAPI (blue). (**B**) Immunolocalisation of UPF1 (red) on polytene chromosomes derived from larvae subjected to a 40 min heat shock at 37°C. UPF1 signals are primarily detected at heat shock gene loci, indicated by their cytological locations (yellow arrowheads), using their standard nomenclature. (**C**) Immunolocalisation of UPF1 (red) at an ecdysone induced transgene (named S136) located at cytological position 63B (yellow line) and the same region on the wild type chromosome after ecdysone treatment. The white dotted lines indicate flanking bands as mapping reference. Chromosomes were stained with DAPI (grey in middle panel or blue in bottom panel).

DOI: https://doi.org/10.7554/eLife.41444.008

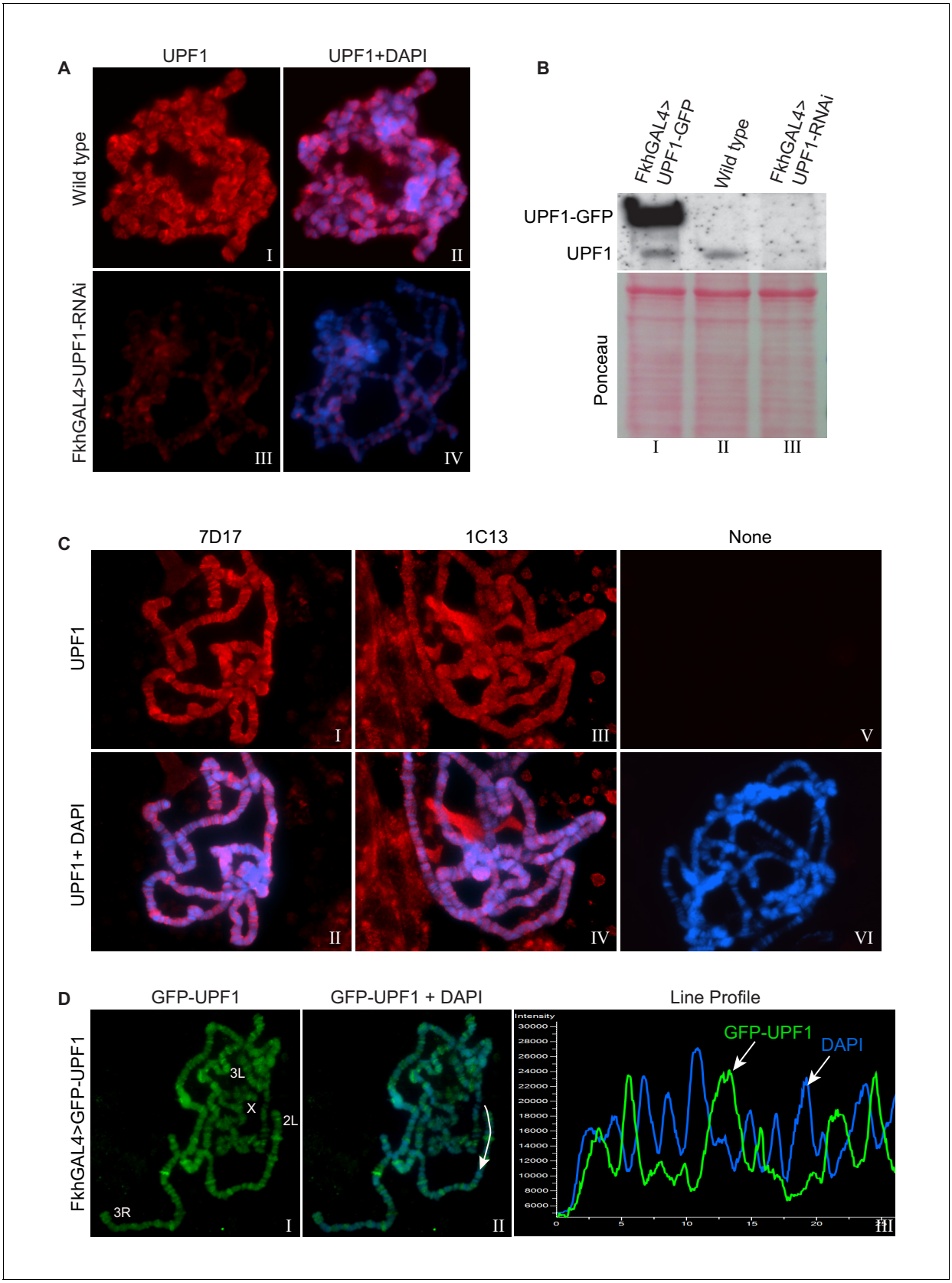

Figure 3—figure supplement 1. RNAi fully depletes UPF1 signal at the salivary gland polytene chromosomes. (**A**) Fluorescence immunolocalisation of UPF1 using the 7B12 monoclonal antibody (Cy3, red) on polytene chromosomes (blue) of wild type (**I, II**) and *FkhGAL4 >UPF1* RNAi (III, IV) salivary

Figure 3—figure supplement 1 continued on next page

Figure 3—figure supplement 1 continued

glands. (**B**) Western blotting probed with 7B12 mab for protein extracts of third instar larval salivary gland from *FkhGAL4 >GFP-UPF1* (lane I), wild type (lane II) and *FkhGAL4 >UPF1* RNAi (lane III). Ponceau staining of the same blot showing equal protein loading. (**C**) Fluorescence immunolocalisation of UPF1 using the two other antibodies described: 7D17 (**I, II**) or 1C13 (**III, IV**) (Cy3, red). No signal is detected on polytene chromosomes in the absence of primary antibody (**V, VI**). (**D**) Immunolocalisation of GFP-UPF1 (FITC, green, (**I and II**) on polytene chromosomes of *FkhGAL4 >GFP-UPF1* salivary glands, detected using anti-GFP antibody. Chromosomes were counter stained with DAPI (blue, **II**). Line profiles in III show both signal intensities along the white line traced on the chromosome arm in II. Note that the UPF1 signal peaks at chromatin-decondensed regions characterised by low DAPI signal.

DOI: https://doi.org/10.7554/eLife.41444.009

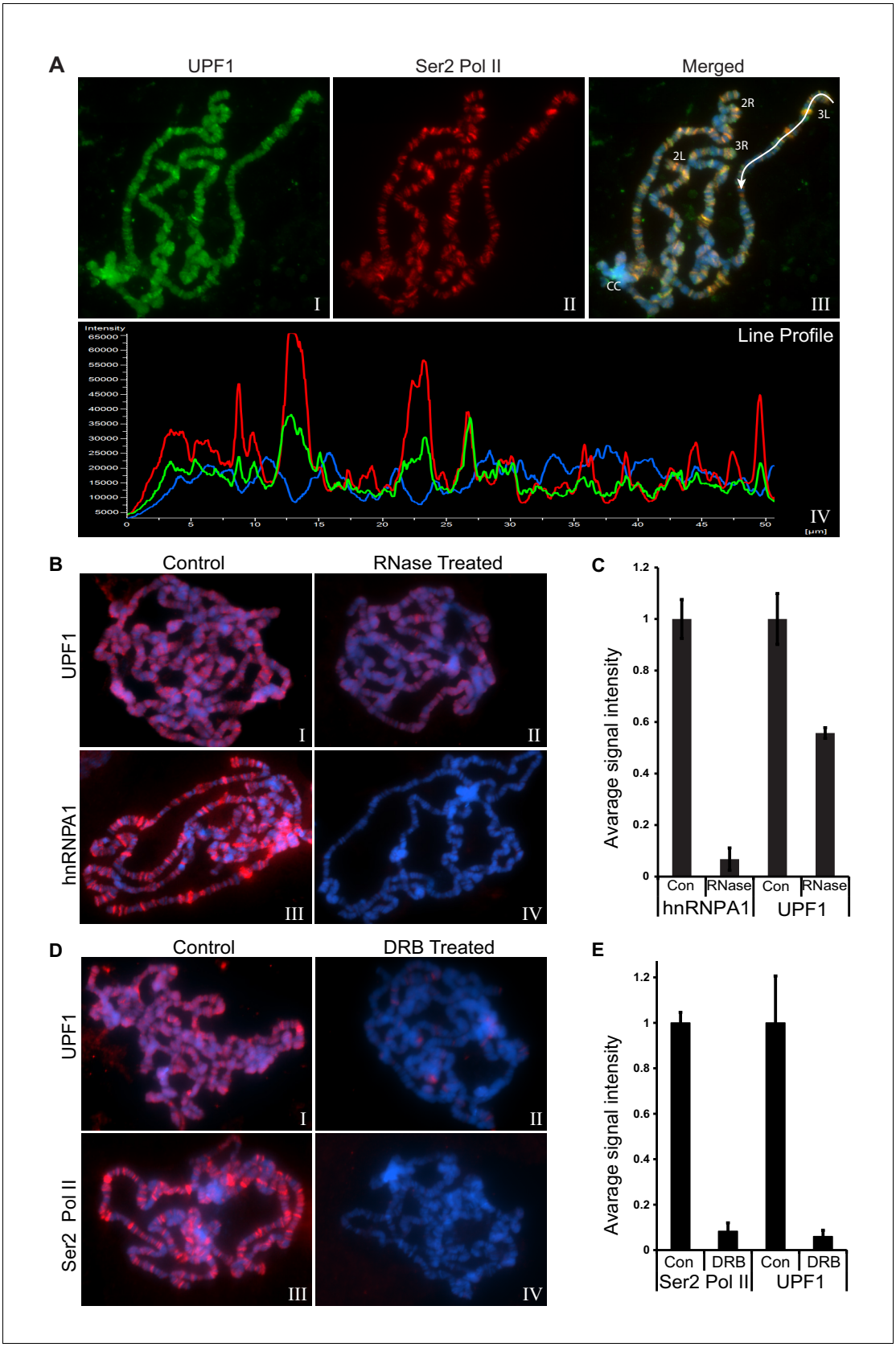

Figure 3—figure supplement 2. UPF1 chromosomal association is transcription and nascent RNA dependent. (**A**) Co-immunolocalisation of UPF1 (FITC, green, I, III) and Ser2 Pol II (Cy3, red, II, III) on polytene chromosomes, counterstained with DAPI (blue). Line profiles in IV show all signal

Figure 3—figure supplement 2 continued on next page

Figure 3—figure supplement 2 continued

intensities along the white line drawn in III. (**B**) Immunolocalisation of UPF1 (red, (**I and II**) and hnRNPA1 (red, **III and IV**) at polytene chromosomes of either untreated salivary glands (**I and III**) or treated with RNase (**II and IV**). (**C**) Graph shows normalised fluorescence intensity of the hnRNPA1 and UPF1 signals in control and after RNase treatment, based on mean intensities of 8–10 different nuclear spreads. (**D**) Immunolocalisation of UPF1 (red, (**I and II**) and Ser2 Pol II (red, **III and IV**) at polytene chromosomes from either untreated salivary glands (**I and III**) or DRB treated (**II and IV**). (**E**) Graph shows normalised fluorescence intensity of Ser2 Pol II and UPF1 in control and after DRB treatment of 8 different chromosomes spreads, based on mean intensities of the signal on all chromosome arms. Error bars in C and E indicate ±Standard Error.

DOI: https://doi.org/10.7554/eLife.41444.010

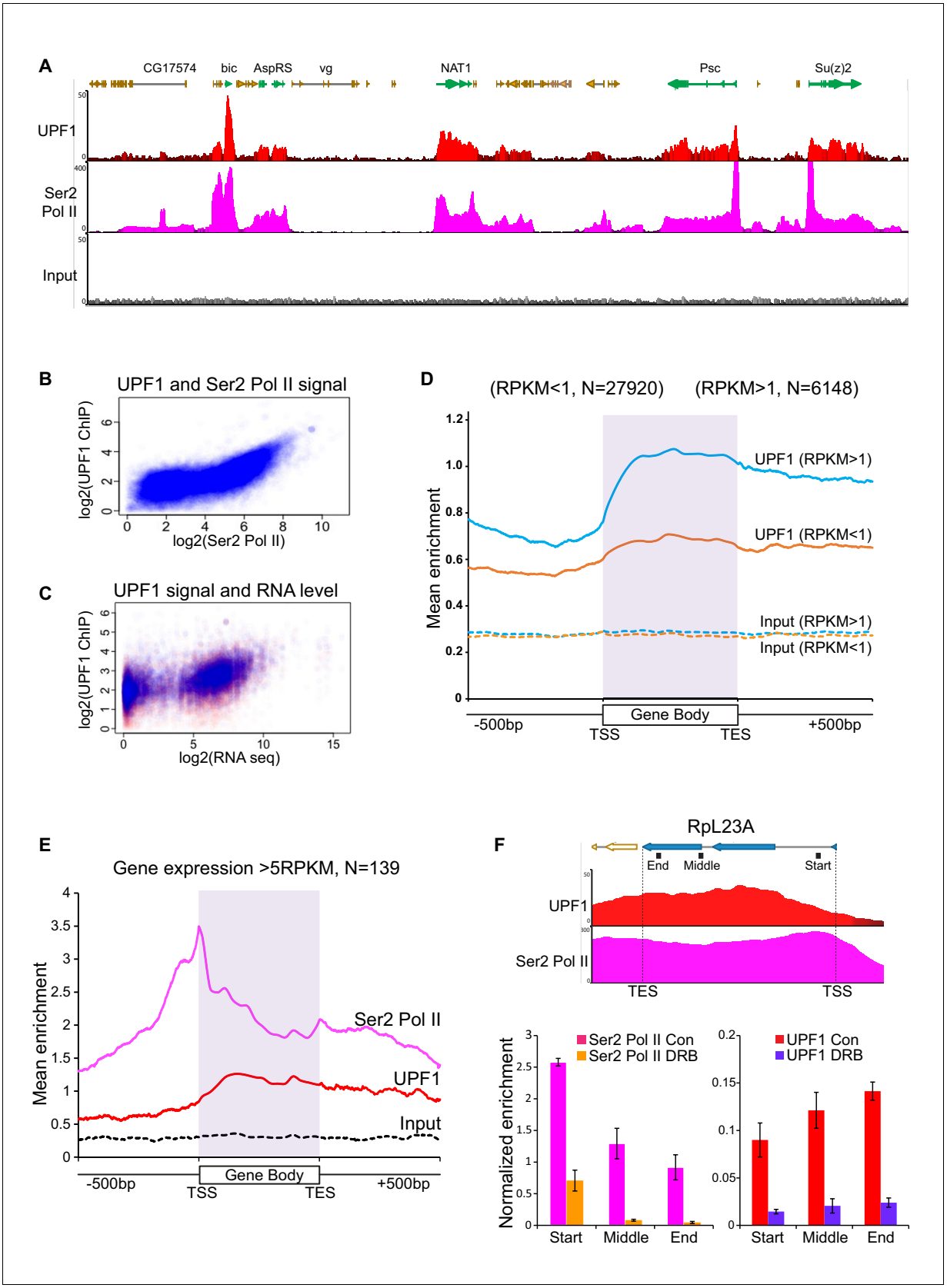

Figure 4. UPF1 associates at Pol II transcription sites. (**A**) Genome browser visualisation of UPF1 (red) and Ser2 Pol II (pink) ChIP-seq enrichment profiles at a representative chromosomal region in S2 cells, including highly active genes (green) and low or inactive genes (orange). The input profile (grey) is

Figure 4 continued on next page

Figure 4 continued

shown in the bottom panel on the same scale as that of UPF1 (**B**) Scatter plot showing correlation between normalised exon reads in UPF1 and Ser2 Pol II ChIP-seq samples. (**C**) Scatter plot showing relationship between normalised UPF1 ChIP-reads vs. mRNA-seq expression levels; data points corresponding to either exons (blue) or introns (red). Correlation values are 0.485 and 0.398, for exons (blue line) and introns (red line) respectively. (**D**) Metagene profiles showing average UPF1 occupancy at either active (blue, RPKM >1) or inactive/low expressed transcription units (RPKM <1, orange), gene body (scaled to 16 bins of gene full length) plus 500 bp from either end. The number of individual transcription units (**N**) used for this analysis is given on top. Corresponding normalised input profiles are shown by dotted lines. (**E**) Superimposed metagene plots of UPF1 (red) and Ser2 Pol II (pink) at highly expressed gene loci (RPKM >5). The input enrichment profile for same gene set is shown by the dotted line (black). (**F**) Graph shows ChIP-seq enrichment profiles of UPF1 (red) and Ser2 Pol II (pink) at the RpL23A gene. Bottom panel shows real-time PCR quantification of Ser2 Pol II (left) and UPF1 (right) average enrichment at RpL23A gene, based on two separate ChIP replicates from either normal or DRB treated S2 cells. The relative position of the three amplicons tested (Start, Middle and End of the gene) are indicated by black boxes underneath the gene schematic on top. Error bars indicate ±Standard Error.

DOI: https://doi.org/10.7554/eLife.41444.011

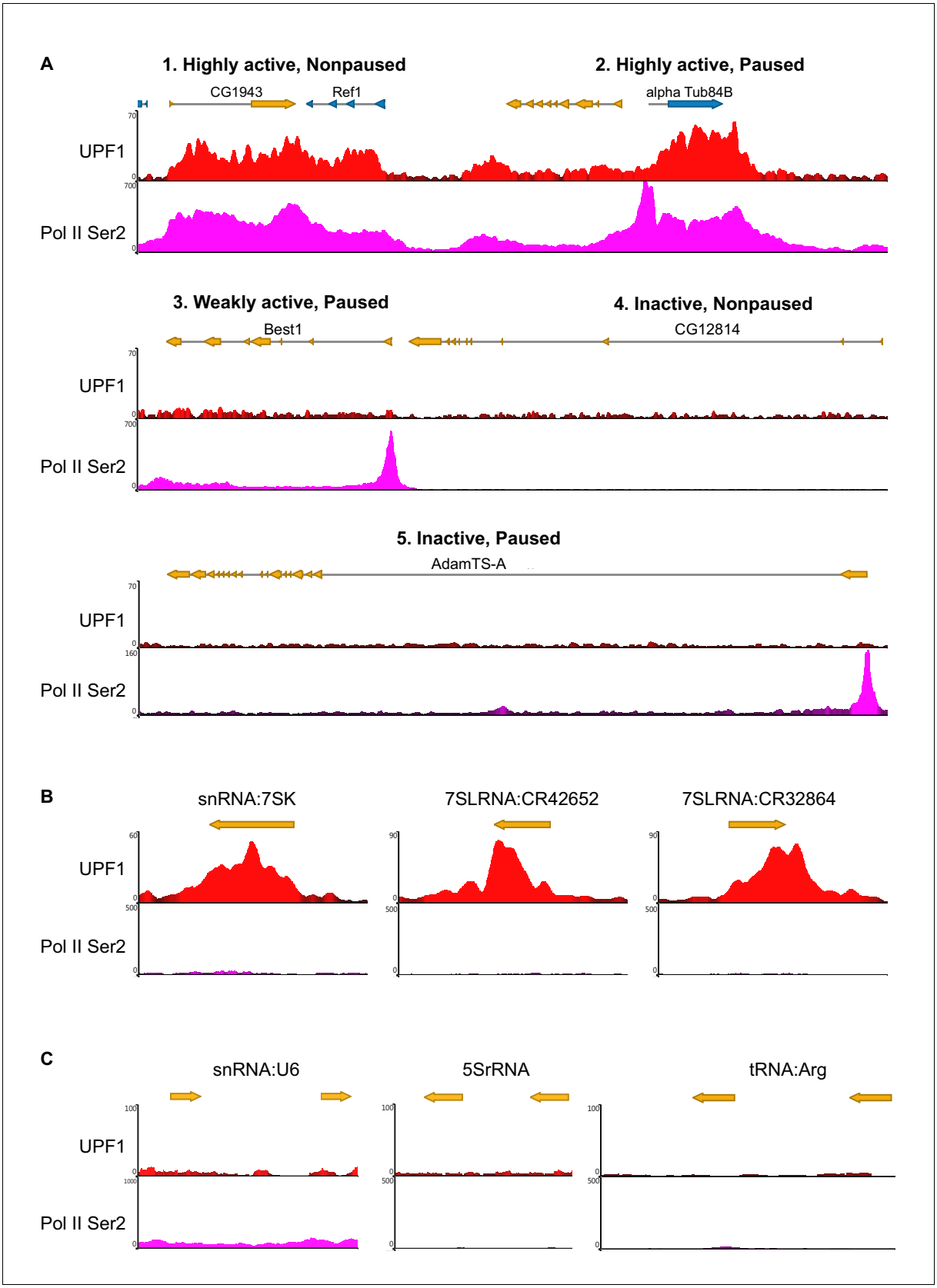

Figure 4—figure supplement 1. ChIP-seq profiles of UPF1 at representative Pol II genes and some Pol III loci. (**A**) ChIP-seq profiles of UPF1 (red) and Ser2 Pol II (pink) at different active genes characterised by either paused or not paused Pol II at the TSS (panels 1–3). Panels 4 and 5 show absence of

Figure 4—figure supplement 1 continued on next page

Figure 4—figure supplement 1 continued

Upf1 at two inactive genes, with or without paused Pol II. (**B**) ChIP-seq profile of UPF1 (red) and Ser2 Pol II (pink) at the three Pol III transcribing gene loci indicated. (**C**) ChIP-seq profiles showing no UPF1 signal at three highly transcribing Pol III genes (snRNPU6, 5SrRNA and tRNA:Arg).

DOI: https://doi.org/10.7554/eLife.41444.013

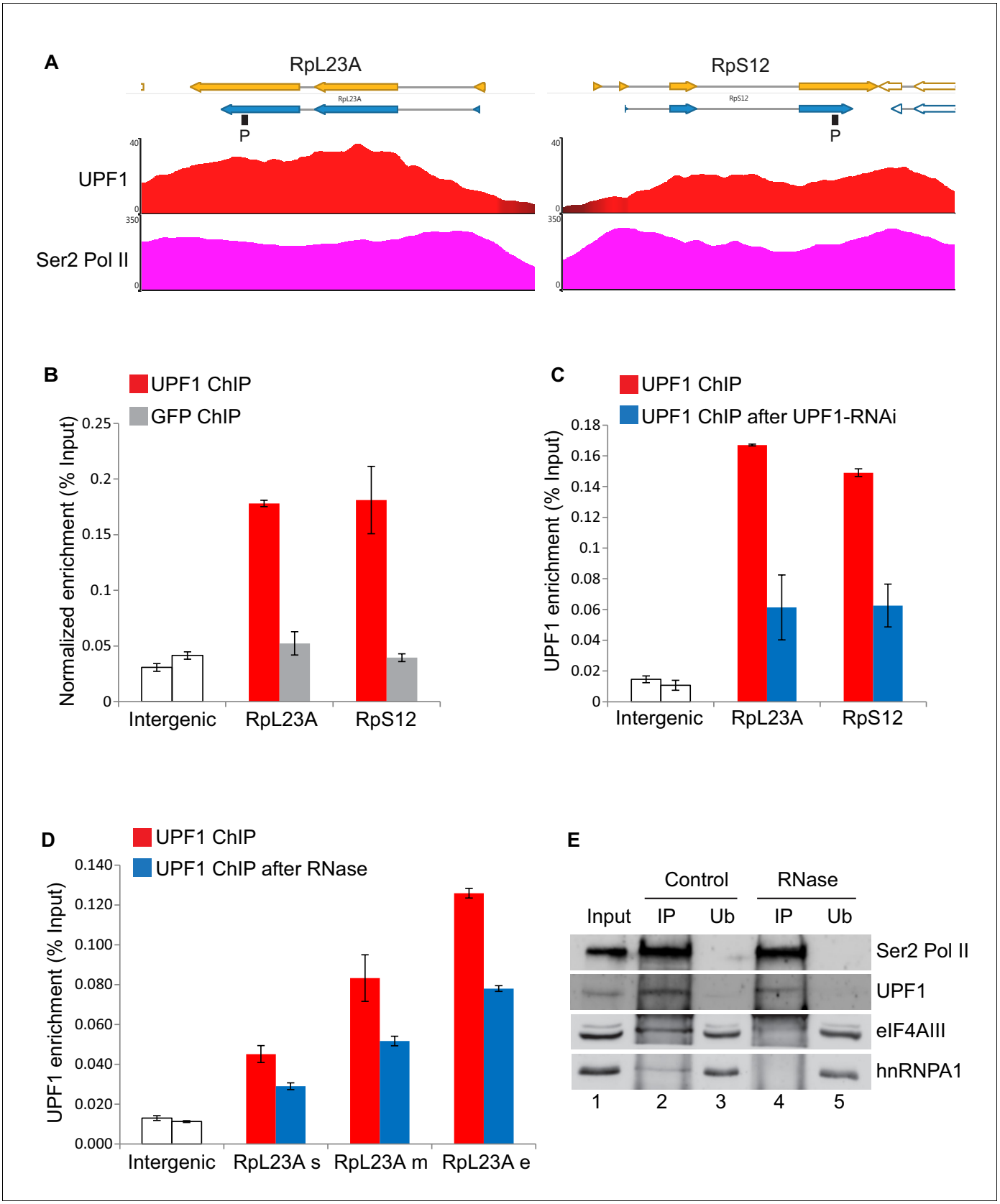

Figure 4—figure supplement 2. Real-time PCR validation of UPF1 ChIP association at selected genes. (**A**) UPF1 (red) and Ser2 Pol II (pink) ChIP-seq enrichment profiles at RpL23A (on left) and RpS12 (on right) gene loci. (**B**) Real-time PCR quantification of average ChIP signal of either endogenous

Figure 4—figure supplement 2 continued on next page

Figure 4—figure supplement 2 continued

UPF1 (red) or GFP (as negative control, grey) at the RpL23 and RpS12 genes in salivary glands expressing GFP. The locations of the primer pairs used are indicated by the black boxes (**P**) shown below the genes schematics in A. (**C**) Real-time PCR quantification of average UPF1 association in control (red) or UPF1-RNAi (blue) S2 cells. (**D**) Real-time PCR quantification of average UPF1 association at three distinct regions of RpL23 in S2 cells (same primers pairs as in ***Figure 4F***), with (blue) or without (red) RNase A treatment. (**E**) Ser2 Pol II immunoprecipitation of S2 cell nuclear extracts using anti-Ser2 Pol II antibody (ab5095) and detection (same blot) of Ser2 Pol II, UPF1, eIF4AIII and hnRNPA1, in control (lanes 2–3) or RNase treated samples (lanes 4–5). IP refers to immunoprecipitated fractions, Ub to unbound fractions. Error bars in B, C and D indicate ±Standard Error.

DOI: https://doi.org/10.7554/eLife.41444.012

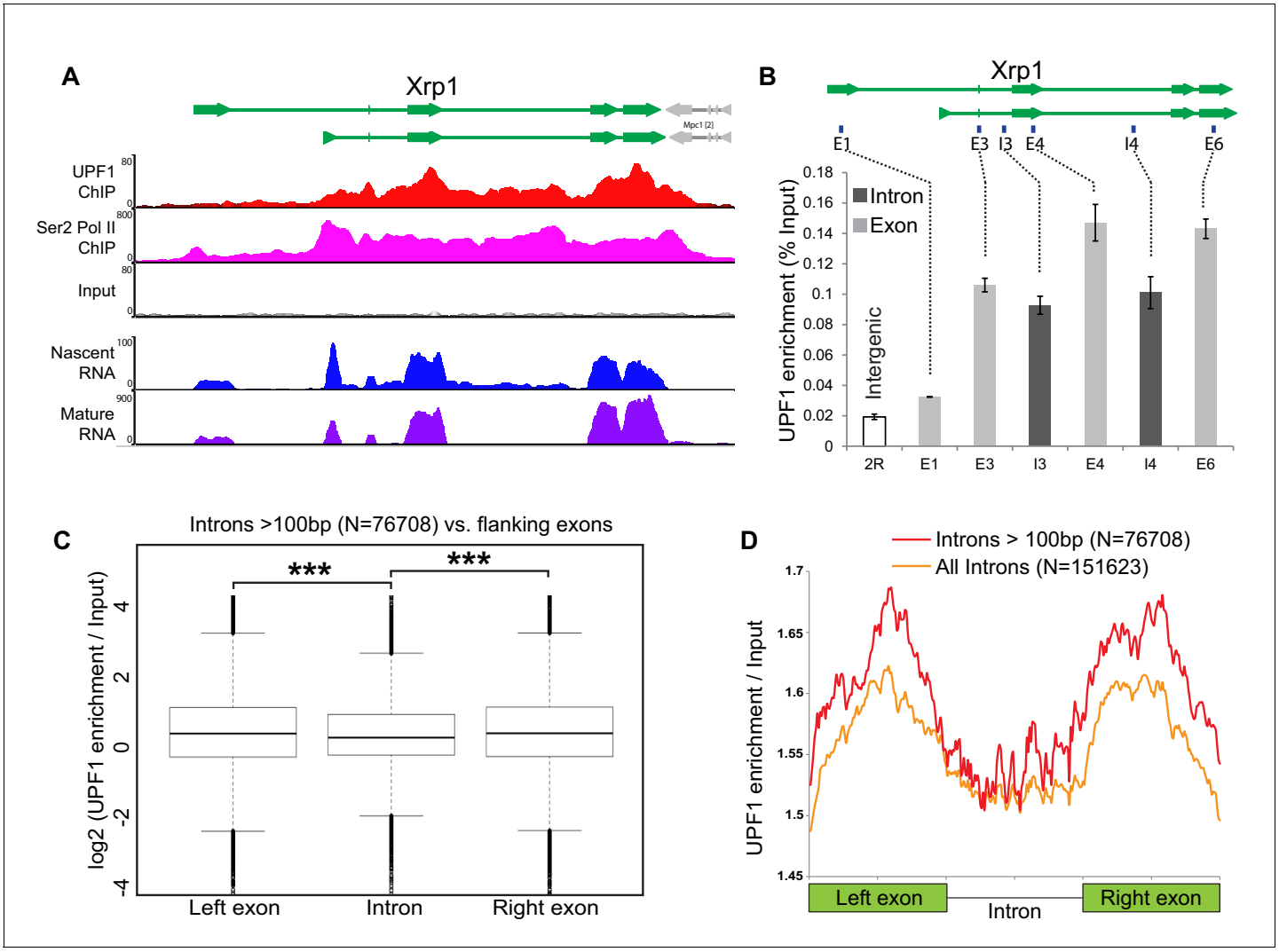

Figure 5. Intron recognition interferes with UPF1 association on nascent transcripts. (**A**) Schematic of the *Xrp1* locus (top) showing its two main transcription units. Below, UPF1 (red) and Ser2 Pol II (pink) ChIP-seq profiles at this gene; that of the input is shown below (grey). The bottom two panels show nascent RNA-seq (blue) and poly(A) RNA-seq (purple) profiles. (**B**) Real-time PCR quantification of average enrichment in different regions in either exons (**E1, E3, E4 and E6**) or introns (I3 or I4) in multiple UPF1 ChIP replicates. Error bars indicate ±Standard Error. (**C**) Box plots of normalised UPF1 ChIP-seq reads mapping at either left exon (shown on left), intron (middle) or right exon (on right). Whiskers correspond to ±1.5 interquartile range with respect to quartiles. Wilcoxon rank sum test values are: left exon vs. intron, p-value=6.737e-08; right exon vs intron, p-value=2.391e-09; and, left exon vs. right exon p-value=0.606. ***p<0.001 for difference in UPF1 signal between intron and its flanking exon. (**D**) Line profile of average UPF1 ChIP-seq/input enrichment expressed as percentage of full length in either exons or intron. Analysis is based on 151623 introns of any length (orange line) or 76708 introns longer than 100 bp (red line) as annotated in the dm6 genome release.

DOI: https://doi.org/10.7554/eLife.41444.014

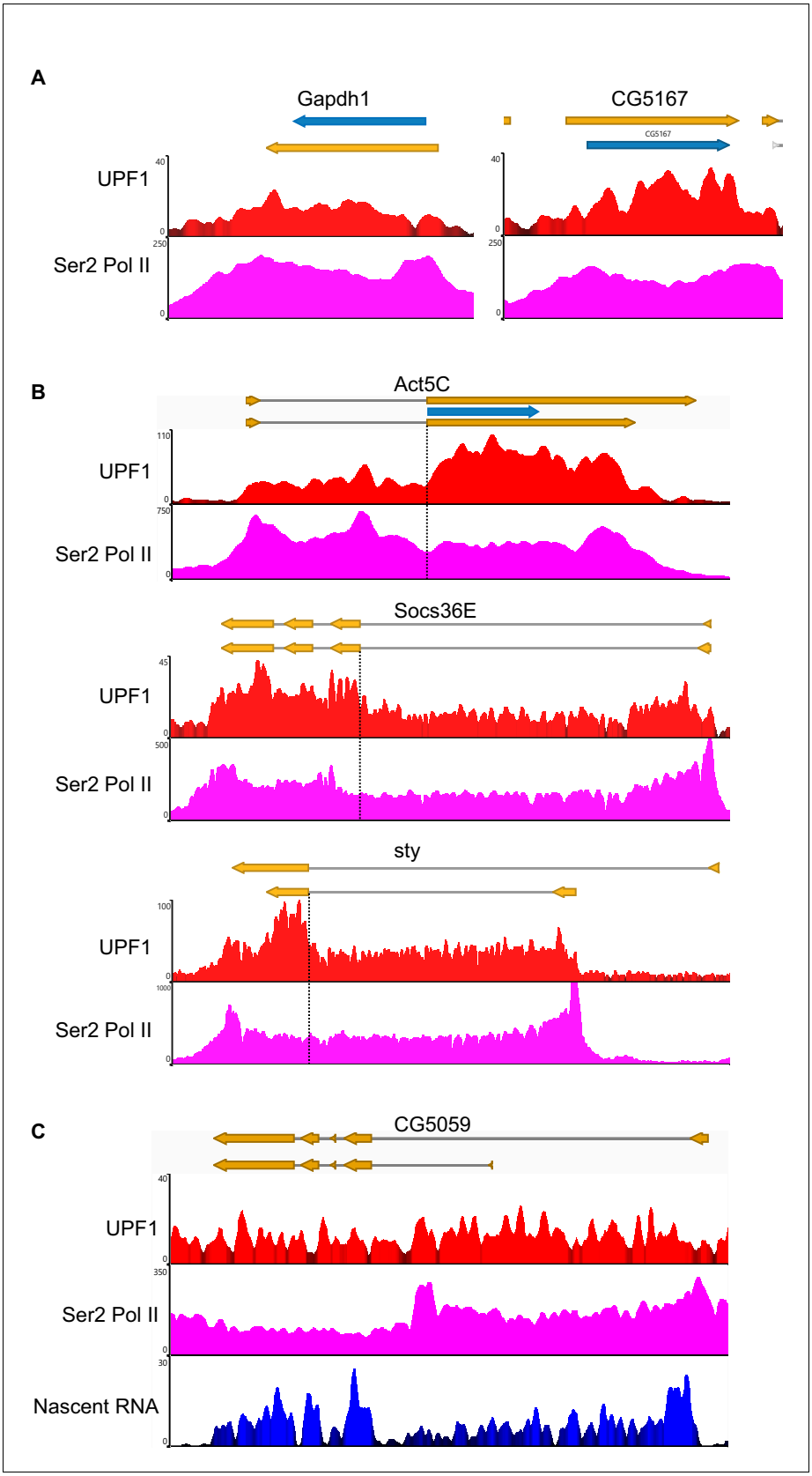

Figure 5—figure supplement 1. Additional examples of UPF1 ChIP-seq profiles at genes with or without introns. (**A**) ChIP-seq profiles showing enrichment of UPF1 (red) and Ser2 Pol II (pink) at genes without intron. Blue arrows indicate their coding sequences (CDS). (**B**) ChIP-seq profile showing

Figure 5—figure supplement 1 continued on next page

Figure 5—figure supplement 1 continued

enrichment of UPF1 (red) and Ser2 Pol II (pink) at other highly expressing intron-containing genes. Dotted lines demarcate regions around intron/exon borders at which UPF1 shows higher association with exons despite uniform Ser2 distribution. The blue arrow in *Actin5C* diagram indicates its CDS. (**C**) UPF1 ChIP-seq profile (red) and Ser2 Pol II (pink) at CG5059 gene, which, as indicated by the nascent RNA-seq profile underneath (blue), show high intronic sequencing reads, indicative of inefficient co-transcriptional splicing.

DOI: https://doi.org/10.7554/eLife.41444.015

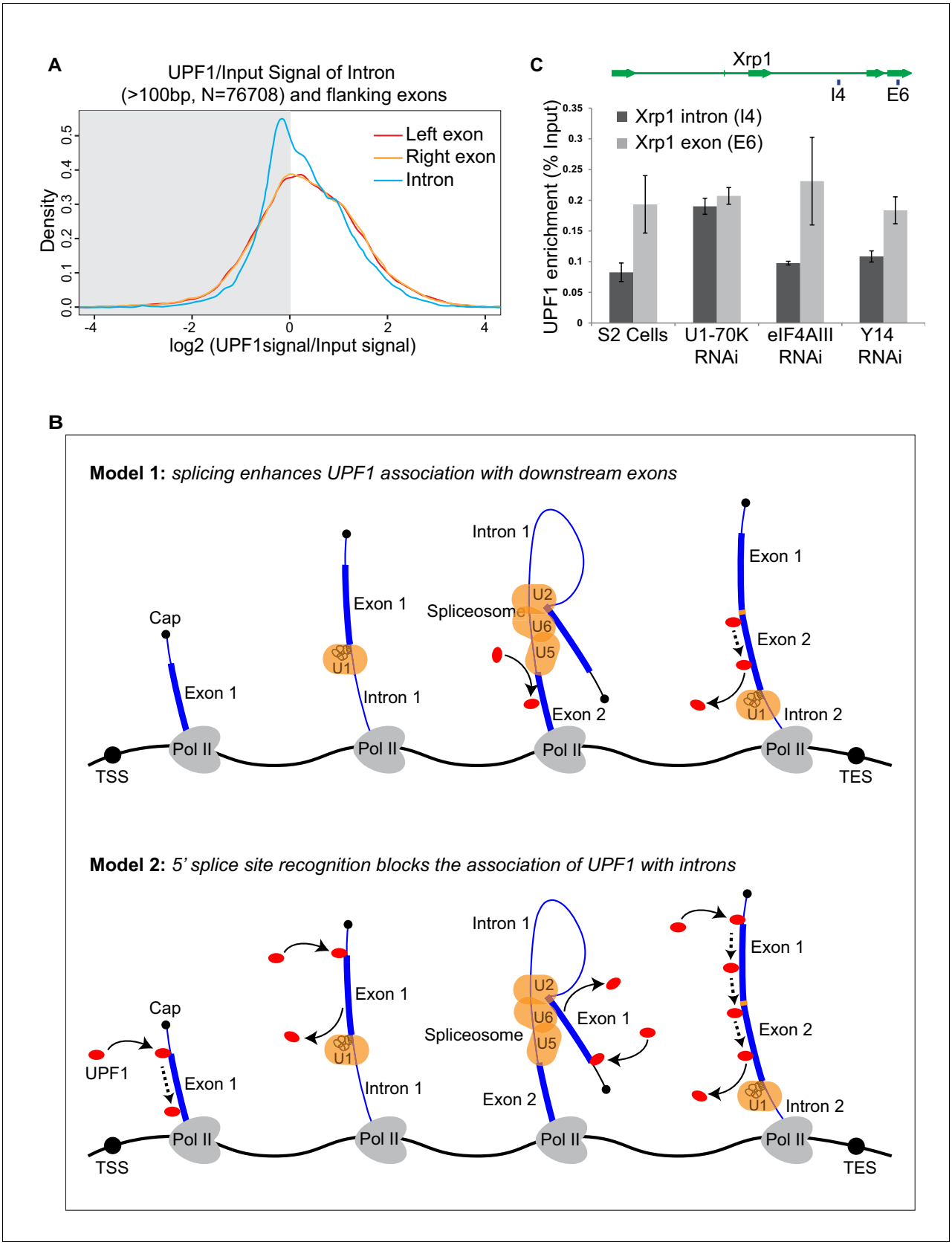

Figure 5—figure supplement 2. UPF1 association with nascent transcripts might depend on 5' splice sites recognition. (**A**) Density plots of UPF1 enrichment at either the exon before (red line), exon after (orange line) or the intron (blue line). The x-axis shows the log2 of the normalised (by input)

Figure 5—figure supplement 2 continued on next page

Figure 5—figure supplement 2 continued

UPF1 ChIP signal; the right half of the graph shows the density of the values that are enriched, the left half (shadowed) those that are not. (**B**) Proposed models of how UPF1 scanning of the nascent transcript is connected to intron recognition during spliceosome assembly: Model 1 (top) predicts that splicing enhances binding of UPF1 to downstream exons, Model 2 (bottom) that intron recognition blocks UPF1 association with introns. Spliceosomal snRNPs (U1, U2/U6 and U5) are represented by orange oval shapes, the squiggle drawing within U1 snRNP signifies the base pairing between U1 snRNA and the 5′ ss; TSS indicate the transcription start site; and TES, the transcription end site. Exons are indicated by either thin blue lines (5′ UTRs) or rectangles (coding regions). (**C**) Real-time PCR quantification of UPF1 ChIP enrichment (two replicates) at intron (**I4**) or exon (**E6**) of the Xrp1 gene, in either normal S2 cells or cells RNAi depleted of the proteins indicated. Error bars indicate ±Standard Error.

DOI: https://doi.org/10.7554/eLife.41444.016

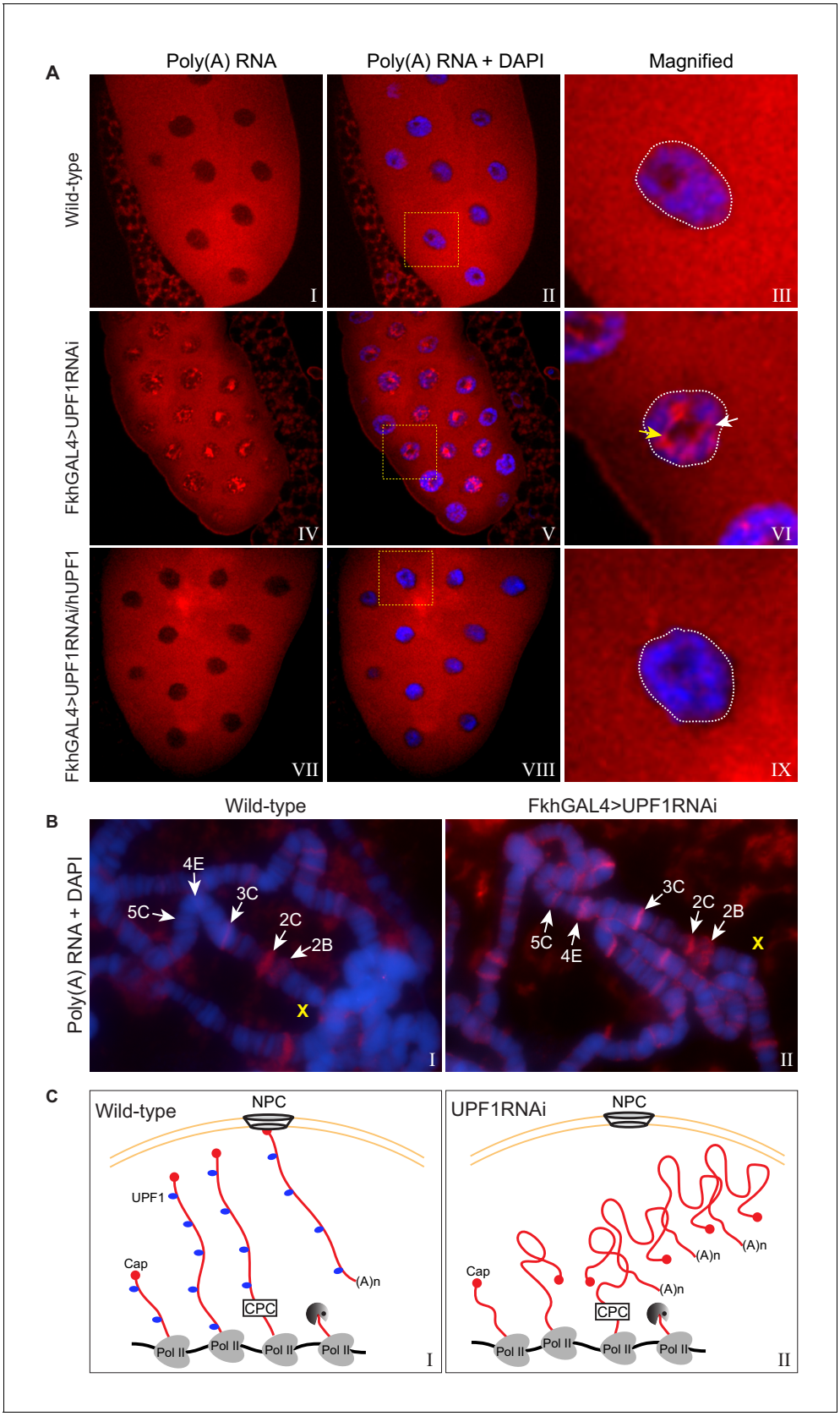

Figure 6. UPF1 knockdown results in nuclear accumulation and transcription sites retention of poly(A) mRNA. (**A**) Fluorescence in situ hybridisation (FISH) with a rhodamine-labelled oligo(dT)45 probe of third instar larval salivary glands, from either wild-type (top panel), UPF1-RNAi (middle panel) or

Figure 6 continued on next page

Figure 6 continued

UPF1-RNAi glands expressing human UPF1 (hUPF1, bottom panel). Chromosomes were counterstained with DAPI (blue). White arrow and yellow arrow indicate interchromosomal and perinucleolar aggregates respectively. (**B**) Oligo(dT)45 FISH (as above) of third instar larval salivary gland polytene chromosomes from either wild type or UPF1-RNAi. Chromosomes were counterstained with DAPI (blue). (**C**) Proposed model of accumulation of newly transcribed poly(A) mRNA at the site of transcription in UPF1 depleted cells (right) compared with wild type (left). Abbreviations: NPC for nuclear pore complex and CPC for cleavage and polyadenylation complex.

DOI: https://doi.org/10.7554/eLife.41444.017